Application of the method of direct mathematical modeling to diamond-shaped contact lines

Sulton Amirov*, *Islom* Karimov, and *Iroda* Abduazimova

Tashkent State Transport University, Tashkent, Uzbekistan

Abstract. The article describes the application of the numerical method to the investigation of the dynamic interaction of contact lines with current collectors of electric rolling stock (ERS).
The law of joint movement of the runner and the contact wire shall be established. If a gap is recorded at any stage, the pressure value is set to zero. From this point on, the flux and contact wire are modeled independently. The contact wire shall be touched by the current collector by the clearance δ. As a rule, the introduction into contact is accompanied by the introduction of a current collector into the contact wire, which is characterized by negative clearance $\delta < 0$. To compensate for the introduction at the point of contact, there must be an additional «push» force defined by the condition of zero clearance at the end of the stage.

1 Introduction

The main way of studying the interaction of the contact suspension with current collectors is currently mathematical modeling. The highest level of detail of the contact suspension is achieved in models developed using the finite element method (FEM) [1, 2], where the suspension is represented by a set of interconnected structural elements, and the movement of each element is described by an ordinary differential equation. Splitting the contact suspension into discrete elements simplifies calculations, eliminating the need to solve partial differential equations. At the same time, there is no need to use any conditional parameters, for instance, the reduced mass of the contact suspension. Sometimes the method of finite differences [3, 4] is used to reduce partial differental equations to a system of ordinary differential equations.

2 Objects and methods of research

Spatial diamond-shaped auto-compensated contact lines (SDACL) have proven to be a design capable of providing stable current transfer to ERS even under the most adverse climatic conditions. Compared with vertical chain suspension, SDACL offers more possibilities for optimizing static properties.

A prospective direction of improvement of methods of studying current collectors, using the FEM principle, is the development of new numerical algorithms on the basis of the method of direct mathematical modeling (DMM) [5].

Calculation of DMM is a powerful tool that allows obtaining simple calculation relations directly, without making differential equations.

* Sulton.amirov@bk.ru

3 Results and their discussion

The use of DMM to solve the problems of the dynamics of the contact network gives a wide range of engineers the opportunity to create mathematical models taking into account the real characteristics of the elements of the contact suspension: contact wire, bearing cable, strings and retainers; to study the interact of contact suspension with several current collectors.

Let's consider the peculiarities of the application of the DMM method to the problems of interaction of contact suspension with current collectors on the example of the spatial diamond-shaped auto-compensated contact network SDACL (Fig. 1). A significant simplification of calculations is achieved by using a flat replacement scheme SDACL, which consists of a contact wire and a bearing cable connected by elastic elements (Fig. 2). In the diagram, the *T* and *K* tension is applied to the suspension wires, equal to the double tension of the carrier cable and the contact wire respectively. The resilient elements are rigid, independent of, the amount of force applied to the retainer, which, according to the results of experiments, is quite reasonable [6-10].

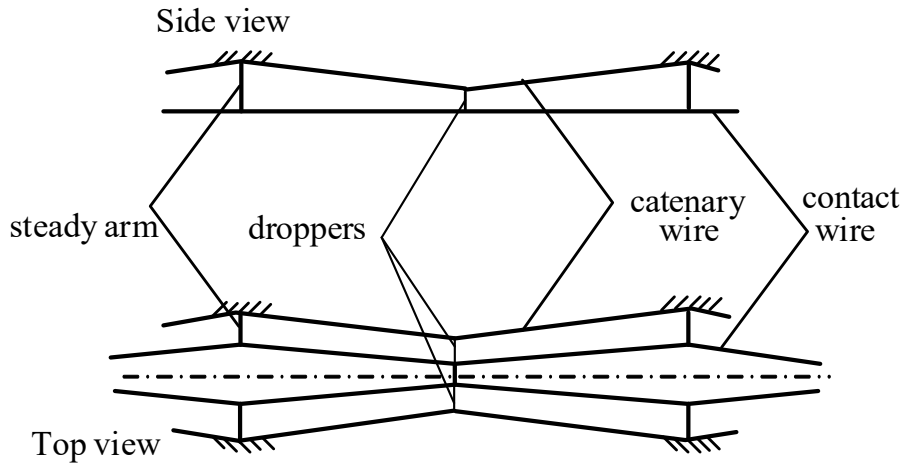

Fig. 1. Location of SDACL elements in the span

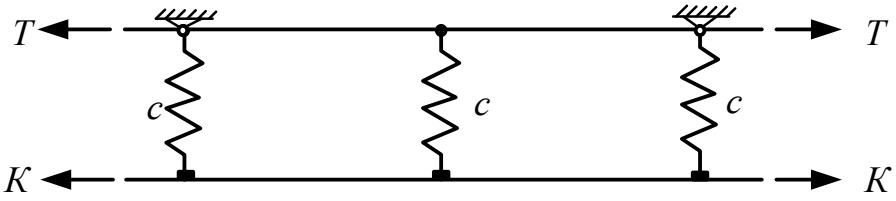

Fig. 2. SDACL flat replacement diagram (single suspension span)

The tension of each of the wires will be considered constant, independent of the pressure of the current collector, and the load from the weight of the contact wires evenly distributed along the span. We will proceed on the assumption that all forces acting on the contact wire are known. In this case, the task is to establish the law of oscillation of the contact wire under the action of several external forces. The full solution to such a problem is given in [5], here we will briefly consider the starting points and basic principles leading to the calculation ratios of the DMM method.

Imagine a contact wire with a completely flexible thread suspended on supports (Fig. 3). Let the suspension points be at the same height level and the distance between the supports is

L. The thread is characterized by linear density ρ and tension *K*.

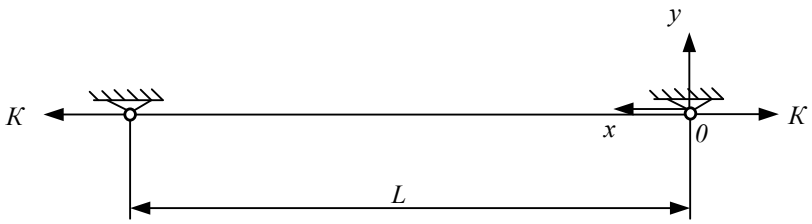

Fig. 3. Elastic thread in original condition

According to the general algorithm of the DMM method, the thread is divided by cross-sections on the *n* composite elements. Both elements and sections are assigned serial numbers. In this case, the number of the left section j must coincide with the number of the element itself. In particular, the first section ($j= 1$) must coincide with the left bound of the filament, and the last ($j= p+ 1$) with the right (Fig. 4, a).

The structural element is conventionally divided into three parts: the inner, which is attributed to the elastic-inertial properties of the element, and the two non-interferential boundary regions.

Each modeling step corresponds to a finite time interval Δt, the duration of which is determined by the expression

$$\Delta t = \frac{\Delta x}{c} .$$

Here is $\Delta x = \frac{L}{n}$ the linear size of the structural element; c –the rate of propagation of transverse waves.

At the beginning of each time stage, the structural element is in a homogeneous state characterized by transverse velocity W_0 and transverse force Q_0 (Fig. 4, b). At this point, the fronts of perturbations (Fig. 4, c) of transverse velocity W and force Q begin to spread from the border to the interior of the element. At the moment of time $0{,}5\Delta t$, the fronts meet in the middle of the element, and when $t > 0{,}5\Delta t$ it is established a homogeneous state, which at the end of the current stage will extend to the entire element.

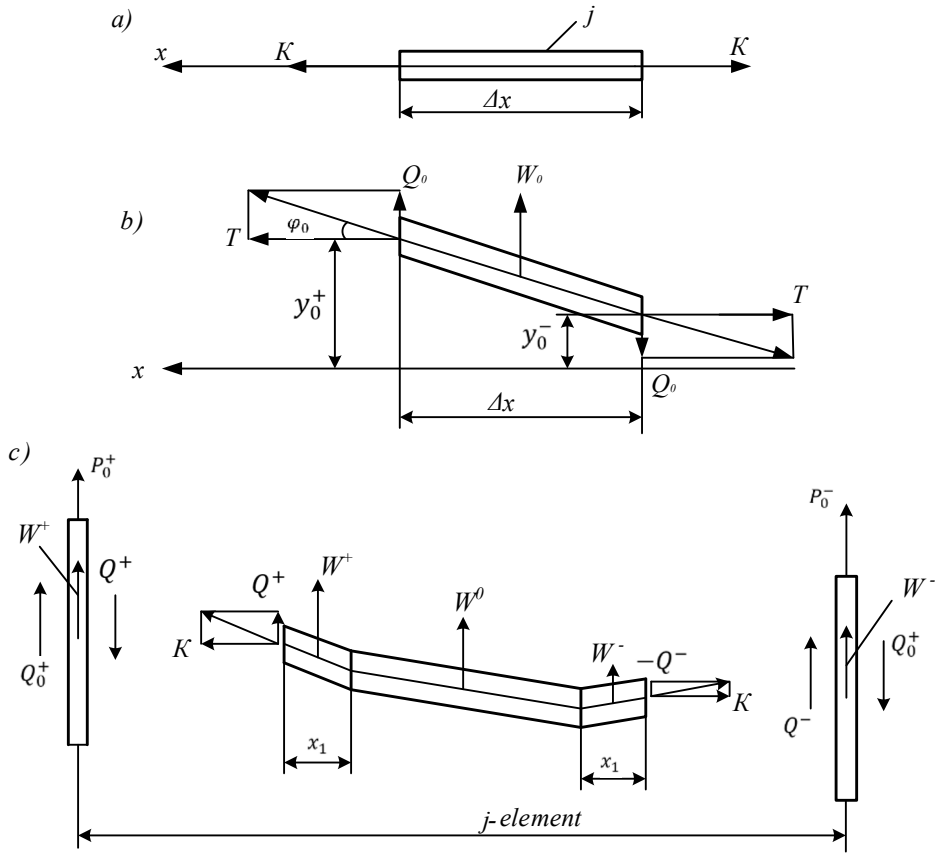

Fig. 4. Final structural element in the original undeveloped state (a), in the propagation of perturbations at the beginning of the current stage (b), in the propagation of perturbations during the time phase (c)

This homogeneous state is characterized by transverse velocity W and transverse force Q

$$W = W_0 + \Delta W^+ + \Delta W^- = W^+ + W^- - W_0 \quad (1)$$

$$Q = Q_0 + \Delta Q^+ + \Delta Q^- = Q^+ + Q^- - Q_0. \quad (2)$$

The increment of the transverse component of the tension is determined by the known K and the tension of the angle tangent increment φ. At small angles φ, the formula is fair

$$\pm K(\varphi^\pm - \varphi_0) = Q^\pm - Q_0 \quad (3)$$

In the propagation of the fronts of perturbations within the structural element, the law of maintaining momentum must be observed

$$Q^\pm - Q_0 = \pm\rho c(W^\pm - W_0) \quad (4)$$

and the condition of continuity

$$W^\pm - W_0 = \pm c(\varphi^\pm - \varphi_0). \quad (5)$$

From expressions (3)-(5) we get

$$c = \sqrt{\frac{K}{\rho}}. \qquad (6)$$

Formula (6) is known to be a classical expression for the velocity of transverse wave propagation in a flexible thread.

Using (1), (2), (4), as well as the conditions of equivalence of transverse velocities and forces on the external boundaries of the structural elements, the recurrent relationships of the DMM method for the flexible thread are obtained:

$$W_j = \frac{W_{j+10}+W_{j-10}+\frac{1}{\rho c}\left[Q_{j+10}-Q_{j-10}+P^{+}_{j^*0}+P^{-}_{j^*0}\right]}{2} \qquad (7)$$

$$Q_j = \frac{\rho c\left[W_{j+10}-W_{j-10}\right] \ +Q_{j+10}+Q_{j-10}+P^{+}_{j^*0}-P^{-}_{j^*0}}{2} \qquad (8)$$

where is $P^{\pm}_{j^*0}$ the force applied to the outer limits of the *j*-th element (Fig. 4).

Determining the transverse velocities and forces of the boundary elements taking into account the equality of zero velocities in the sections $j = n+1 \quad (W_1^- = 0, \ W_n^+ = 0)$, we arrive at the following ratios:

$$W_1 = \frac{W_{20}-W_{10}+\frac{1}{\rho c}\left[Q_{20}-Q_{10}+P^{+}_{1^*0}\right]}{2} \qquad (9)$$

$$W_n = \frac{W_{n-10}+W_{n0}-\frac{1}{\rho c}\left[(Q_{n-10}-Q_{n0})-P^{-}_{n^*0}\right]}{2} \qquad (10)$$

$$Q_1 = \frac{\rho c\left[W_{20}+W_{10}\right] \ +Q_{20}+Q_{10}+P^{+}_{10}}{2} \qquad (11)$$

$$Q_n = \frac{\rho c\left[W_{n-10}+W_{n0}\right]-(Q_{n-1}+Q_{n0})+P^{-}_{n0}}{2}. \qquad (12)$$

Expressions (7) - (12) form a complete system of recurrent relationships of the DMM method for a flexible thread. The simulation is limited to determining the values of the transverse velocities and forces at the current time stage by substitution in (7) to (12) known external forces, as well as the parameters of the capital Q_0 and W_0, determining the state of each element at the previous stage.

Figure 5 shows the contact wire profiles obtained by computer simulation. This is the result of a simulation. Here, a concentrated vertical force of 120 N is applied to the contact wire in a 25 m span at a speed of 200 km/h (69.44 m/s). Contact wire tension 15 kN, linear density 1.068 kg/m. The curves $t_1 - t_3$ illustrate the position of the contact wire respectively at times 0.0644 s, 0.0862 s, and 0.1165 s.

Before meeting the right border, the wavelength of the front is close to straight. The inclination angle of this line to the *x* is determined by the ratio of the current collector speed and the perturbation propagation rate. So, if these speeds were equal, the wave front would be a line perpendicular to the *x*.

Based on the data obtained by simulating the variation of the flexible strand under the action of concentrated force, one of the phenomena observed in practice is explained: It has been determined that with the increase in the speed of movement of the current collector, the point of the maximum release of the contact wire shifts in the direction of travel. It is easy to notice that the trajectory of the point of contact is close to the line until the moment of meeting with the front of the wave reflected from the right border (the curve $t_1 and \ t_2$). At this point begins a sharp decline of the contact point (curve $t_1 and \ t_3$), caused by the overlap of the reflected wave. Therefore, the higher the velocity, the farther the current collector moves until the moment of meeting with the front of the reflected wave and the closer the point of the greatest push to the right border.

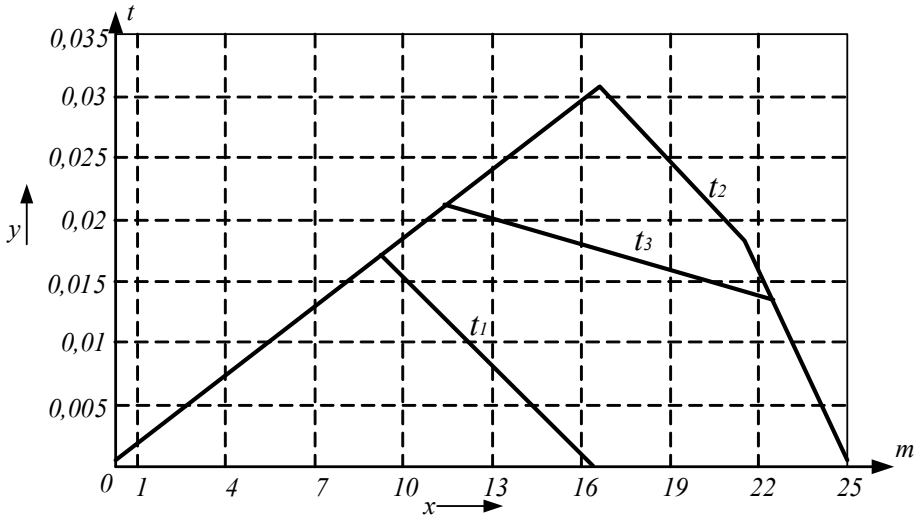

Fig. 5. Flexible thread under movable load

In general, the value of $P_{j^*0}^{\pm}$ equals the sum of the projection forces on the y-axis applied to the outer limits of the elements. In the above example, $P_{j^*0}^{\pm}$ determines the amount of pressure of the current collector on the contact wire. It is known that during the interaction of the contact suspension with the current collectors, the pressure is not constant and can vary widely. If during the time interval Δt between the contact wire and the runner of the current collector, there is a gap ($\delta > 0$), pressure equals zero, and the suspension makes free fluctuations. When the flow collector slides along the contact wire ($\delta = 0$), the suspension oscillations should be considered as forced, caused by the force of the current collector. In order to determine this force, let's think of the canopy as a point mass *m* on which the vertical force F_T. Suppose that at the end of the sometimes stage the mass *m* moved vertically upwards towards the wire at a speed W_{m0}. Assuming that during the next time stage, the mass is in contact with the wire, we get the formula to determine the average, within a stage, speed

$$W_{ml} = W_{m0} + 0.5\Delta W_m = W_j^- = W_{j-1}^+ \qquad (13)$$

here $W_m$is the full-speeded change during the stage.

Since the mass *m* of at moves in contact with the wire, the average speed W_{av} is equal to the speed of the boundary of the elements at the point of contact

$$W_{av} = W_j^- = W_{j-1}^+.$$

According to the law of maintaining momentum

$$\Delta W_{av} = F\frac{\Delta t}{m} \qquad (14)$$

here $F = F_H + F_T$ - the *y*- axial projection of equivalently applied external forces to the mass *m*; $F_H = Q_j^- - Q_{j-1}^+$ - the projection oy-axis of the force acting on the mass *m* of the wire. The force of the capital F_H is equal in absolute value and is opposite in direction of the force of contact pressure.

Using (4), we get

$$Q_j^- - Q_{j-1}^+ = Q_{j0} - Q_{j-10} - \rho c[2W_j^- - (W_{j0} + W_{j-10})].$$

Considering (13) and (14), come to the expression

$$F_j = \frac{Q_{j0} - Q_{j-10} - \rho c[2W_{m0} - (W_{j0} + W_{j-10})] - F_T \frac{m_j}{m}}{1 + \frac{m_j}{m}} \qquad (15)$$

here $m_j = \rho c \Delta t$.

The ratios (7)-(12), (15) establish the law of joint movement of the runner and the contact wire. If a gap is recorded at any stage, the pressure value is set to zero. From this point on, the flux and contact wire are modeled independently. The contact wire is touched by a screw-flow collector and monitored by the amount of delta clearance δ. Normally, the introduction of a current collector into a contact wire, which is characterized by a negative delta clearance $\delta < 0$, is accompanied by an additional "expander" to compensate for the introduction at the contact point of the force defined by the zero-gap condition at the end of the step.

4 Conclusions

Fig. 6 shows the profiles of the contact wire interacting with the current collector. It is a traditional system with two degrees of freedom. The mass of the runner is 16.7 kg, and the mass of the movable frame system is reduced to the top hinge is 15.8 kg. The rigidity of the top unit is 6.0 kN/m. The static pressure of 120 N. At the time t = 0, the current collector was under the left base point (x = 0) and had an initial speed of 200 km/h, which remained constant throughout the simulation.

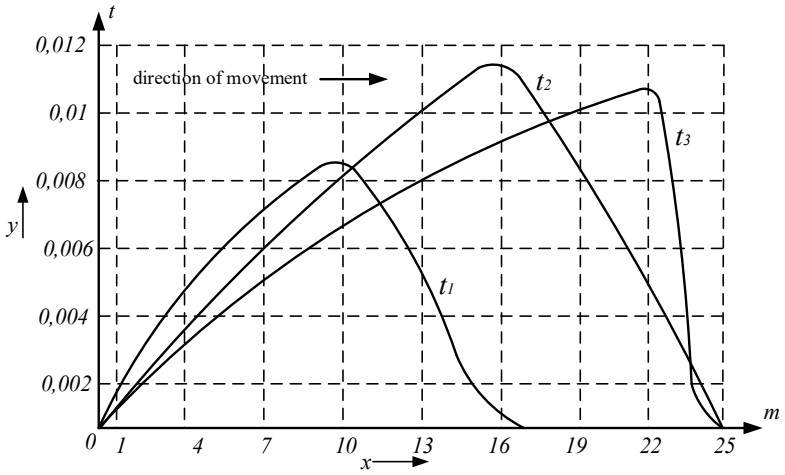

Fig. 6. Spread of disturbances in the contact wire caused by the influence of the current collector

It is obvious that the use of the current collector in the calculation of the model leads to a significant change in the results compared to the earlier case (Fig. 5). For example, the shape of the fronts is significantly affected by the mass of the current collector, and the deviation of the contact pressure from the static effect - on the amount of maximum release of the contact wire.

References

1. Demchenko A.T. Turkin V.V. Application of the method of direct mathematical modeling to the study of the dynamics of contact suspension. Science and technology of transport, Vol. 3. (2004).
2. Fisher B. Chain Contact Suspension and High-Speed Current Collector// World Railways, Vol. 7. (1978).
3. Petri K., and Wallachek J. Modelling the Dynamic Behaviour of Catenary Pantograph Systems for High Speed Trains. Proceedings of Cable Dynamics. (1995).
4. Petri K., and Wallaschek J. Analytical models for the dynamics of catenary-pantograph systems. Zeitschrift für angewandte Mathematik und Mechanik, Vol. 76, pp. 381-382. (1996).
5. Garg V. Dynamics of railway vehicle systems. Elsevier. (2012).
6. Li L., and Chen G. Simulation of high-speed pantograph dynamic performance based on finite element model and aerodynamic pantograph model. In Journal of Physics: Conference Series, Vol. 1064, No. 1, p. 012027. (2018).
7. Bayanov I., Badretdinov T., Muminov S., Karimov I., Saydivaliev S., and Saliyev E. The electric field of the sliding contact during the interaction of the pantograph and the contact wire. In E3S web of conferences, Vol. 264, p. 04029. (2021).
8. Yakubov M., Turdibekov K., Sulliev A., Karimov I., Saydivaliyev S., and Xalikov S. Improvement of the information-measuring complex for diagnostics of traction power supply objects at high-speed traffic. In E3S Web of Conferences, Vol. 304, p. 02014. (2021).
9. Shudong W., Jingbo G., and Guosheng, G. Research of the active control for high-speed train pantograph. In 2008 IEEE Conference on Cybernetics and Intelligent Systems, pp. 749-753. IEEE. (2008).
10. Zheng T. Q., Wu Y., and Zheng J. H. Optimizing active control scheme of high-speed pantograph. In 2009 IEEE 6th International Power Electronics and Motion Control Conference, pp. 2622-2626. IEEE. (2009).